# V Applications of DNS

The particle movers created in our Grand Challenge project were designed to (1) simulate the remarkably different flow microstructures which arise from particle-particle and particle-wall interactions in Newtonian and viscoelastic fluids, and (2) determine the effects of these microstructures on anisotropic and other properties of flowing suspensions. These are computational studies of scale and structure; how do the effects of microstructure at the particle level scale into flow effects at the slurry level?

## ▪ Studies of Microstructure

There is a microstructure which is induced by the fluid dynamics of moving bodies and is governed by a very simple principle: Long bodies are stable across the stream in Newtonian fluids but along the stream in viscoelastic fluids (figure V.1). A key to understanding microstructure in flowing suspensions of spherical bodies is the stable orientation of long bodies and pairs of spherical bodies in momentary contact, Fortes, Joseph and Lundgren 1987, Hu 2001, Huang, Feng and Joseph 1994, Huang, Hu and Joseph 1998, Joseph 1993, Joseph 1996, Joseph, Fortes, Lundgren and Singh 1987, Leal 1980, Liu and Joseph 1993, Singh, Caussignac, Fortes, Joseph and Lundgren 1989.

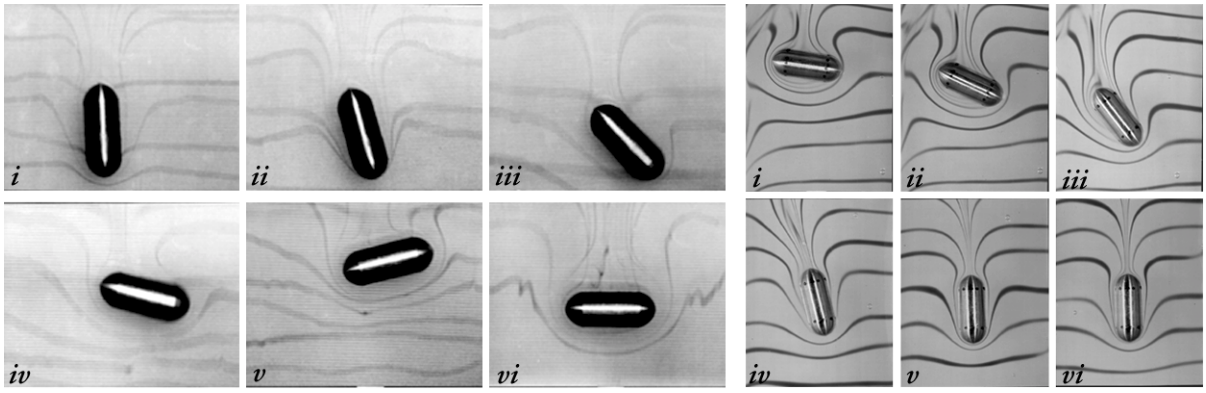


*Figure V.1: Cylinders falling in (a) Newtonian fluid (glycerin), and (b) viscoelastic fluid (2% polyox in water). In glycerin, the cylinder is turned to the horizontal by inertia; in polyox, it is turned vertical by viscoelastic pressures.*

Particle pair interactions are fundamental mechanisms that enter strongly into all practical applications of particulate flows. They are due to inertia and normal stresses and they appear to be maximally different in Newtonian and viscoelastic liquids. The principal interactions between neighboring spheres can be described as *drafting, kissing,* and *tumbling* in Newtonian liquids (figure V.2a) and as *drafting, kissing*, and *chaining* in viscoelastic liquids (figure V.2b). The drafting and kissing mechanisms involved are distinctly different, despite appearances, Fortes *et al* 1987, Glowinski, Pan, Hesla, Joseph and Périaux 1998, Hu 2001, Joseph 1993, Joseph 1996, Joseph, Fortes, Lundgren and Singh 1987, Joseph and Liu 1995, Joseph, Liu, Poletto and Feng 1994, Liu and Joseph 1993.

In Newtonian liquids, when one falling sphere enters the wake of another, it experiences reduced drag and *drafts* downward into *kissing* contact with the leading sphere. The two kissing

spheres momentarily form a single long body aligned parallel to the stream. But the parallel orientation for a falling long body is unstable: hydrodynamic turning couples tend to rotate it to the broadside-on orientation (perpendicular to the stream). The pair of kissing spheres therefore *tumbles* to a side-by-side configuration. Two touching spheres falling side-by-side are pushed apart until a stable separation distance between centers across the stream is established, Joseph 1996, Joseph, Liu, Poletto and Feng 1994, Singh *et al* 1989; they then fall together without further lateral migrations.

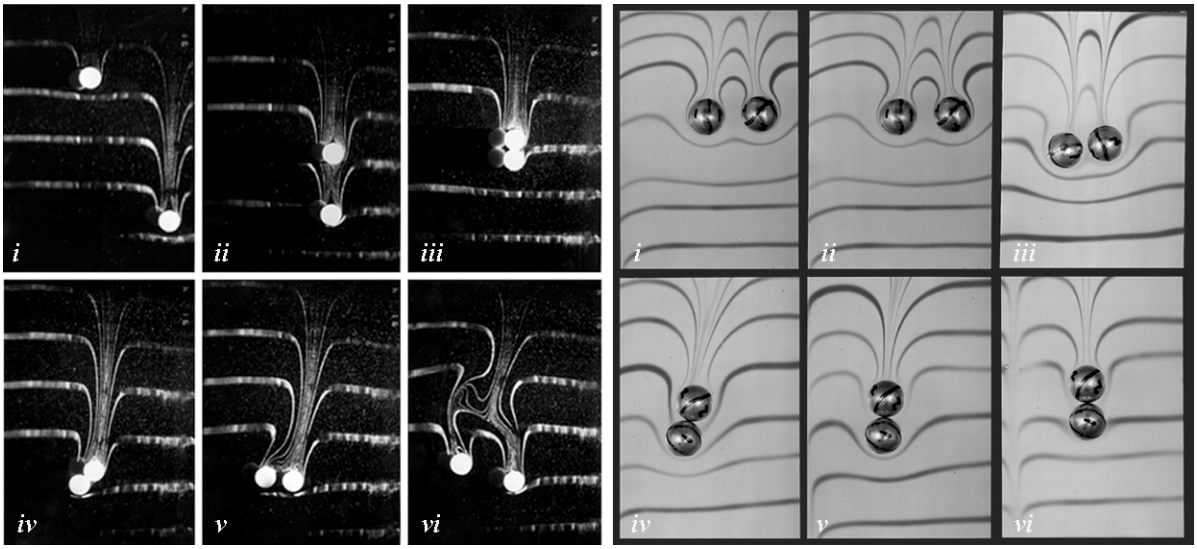


*Figure V.2: (a) Spheres in Newtonian Fluids. Spheres fluidized in glycerin draft (i–ii), kiss (iii), and tumble (iv–vi). They tumble because a pair of kissing spheres acts like a long body, which is unstable when its long axis is parallel to the stream. The forces in a Newtonian fluid are dispersive; the tumbling spheres are pushed apart (v–vi). (b) Spheres in non-Newtonian Fluids. Spheres falling in 2% polyox in water draft, kiss, and chain. They chain because the forces in a viscoelastic fluid are aggregative. A chain of spheres acts like a long body, which is stable with its long axis vertical. The chained spheres turn just like the solid cylinder in figure V.1b (i–vi). Reversing time, we see that chaining, kissing and drafting in V.2b (vi–i) are like drafting, kissing, and tumbling in V.2a (i–vi)*

This local rearrangement mechanism implies that globally, the only stable configuration is the one in which the most probable orientation between any pair of neighboring spheres is across the stream. The consequence of this microstructural property is a flow-induced anisotropy, which leads ubiquitously to lines of spheres across the stream; these are always in evidence in two-dimensional fluidized beds of finite-size spheres, Joseph 1993, Singh, Caussignac, Fortes, Joseph and Lundgren 1989 (see figure V.3a). In viscoelastic liquids, on the other hand, two spheres falling one behind the other will be pushed apart if their initial separation exceeds a critical value. However, if their initial separation is small enough, they will attract ("draft"), kiss, turn and chain, as shown in figure V.2b. One might say that we get dispersion in a Newtonian liquid and aggregation in a viscoelastic liquid, Hu 2001, Hu, Joseph and Fortes 1992b, Joseph 1993, Joseph 1996, Joseph and Liao 1994, Riddle, Narvaez and Bird 1977.

Many stable arrangements—i.e., steady particulate flows—like the "birds in flight" shown in figure V.3c, and some bizarre steady arrangements of 2, 3, and 4 long cylinders (stable doublets, triplets, and quadruplets, Joseph 1993, Joseph 1996) are seen in thin fluidized beds. The

arrangements displayed in figures V.1–3 have never been acknowledged in any two-fluid or mixture-theory model of particulate flow. **These models cannot predict such arrangements because no provision is made for the forces that turn long bodies across or along the stream; hence, two-fluid and mixture theory are silent about microstructur**e. This certainly is a motivation for DNS, and suggests new challenges for mathematical analysis and two-phase flow modeling.

(a) (b) (c)

*Figure V.3: Stable arrays of spheres in (a) Newtonian, and (b) viscoelastic fluids. (a) Fourteen spheres line up in a robustly stable array across the stream of a Newtonian fluid in a fluidized bed. (b) Seven and four spheres fall in a viscoelastic fluid with their long axis vertical and parallel to the stream, stably and permanently chained. (c) Spherical particles in a Newtonian fluid form like* ***birds in flight****. When 22 < Re < 43, the spheres do not draft, kiss, and tumble. Three and four of them form a permanent nested wake structure in which each successive sphere is nested in the wake of the one before and rotates in a shear field there.*

Particle-wall interactions also produce anisotropic microstructures in particulate flows, such as clear zones near walls, and the like. If a sphere is launched near a vertical wall in a Newtonian liquid, it will be pushed away from the wall to an equilibrium distance at which lateral migrations stop. There is also an equilibrium distance for viscoelastic liquids to which spheres will always migrate; this distance is often so close to the wall that spheres appear to be sucked all the way to the wall, Huang Feng, Hu and Joseph 1997, Joseph, Liu, Poletto and Feng 1994. These microstructural features ought ultimately to enter into understanding and control of the lubrication of slurries.

We showed by mathematical analysis Huang, Hu and Joseph 1998, Joseph and Feng 1996, and Joseph 1996 that the normal stresses on a rigid body in a viscoelastic fluid give rise to a "viscoelastic pressure" proportional to the square of the shear rate at the particle boundary, which is large where the velocity is large and zero at stagnation points where the pressure due to inertia is largest. Thus, the viscoelastic pressure is large where the inertial pressure is small and vice-versa, so that the turning couple on a long body has the *opposite* sign in a viscoelastic fluid than it has in a Newtonian fluid—the body aligns *parallel to* the stream. Viscoelastic pressures are compressive everywhere and tend to impel nearby bodies together (figure V.2b) whereas the stagnation point pressures act at points toward the inside of near bodies and tend to push them apart (figure V.2a). The pressures due to viscoelasticity are aggregative, gluing together the long chain of spheres in figure V.3b. The chain is stable because it is a long body aligned with the stream. The pressures of inertia are dispersive so that the array of spheres across the stream in figure V.3a are permanently separated.

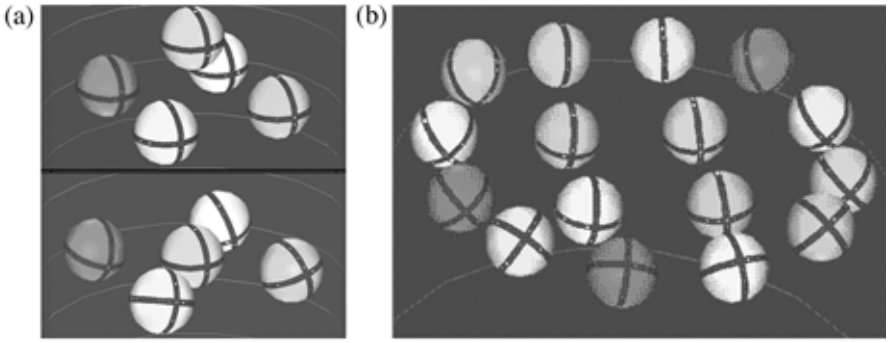


*Figure V.4: Planes of falling spheres across the stream in a tube computed by the ALE particle mover. (a) Five spheres (Re = 45); four are in a horizontal plane. The center sphere oscillates on the center line relative to the plane. (b) Sixteen spheres (Re = 20) in two rings in a plane across the flow.*

Most of the microstructural features just mentioned have been simulated by the ALE particle mover. Some new arrangements are predicted. In the simulation of 5 spheres sedimenting in a tube shown in figure V.4a, 4 of the spheres fall stably in a planar array perpendicular to the stream, which fits well with the fact that the stable orientation of a long body is perpendicular to the stream. The center sphere, however, does not remain in the plane; it either escapes by dropping through the others, or oscillates back and forth across the plane of the other 4, along the center line. This is a particle-flow realization of leapfrogging vortex rings. The sedimentation of 16 spheres leads to two rings of spheres in a plane perpendicular to the stream (figure V.4b).

Chaining appears in our simulations, and it does not destroy the mesh between particles, even in some cases when no special collision strategy is used, Feng, Huang and Joseph 1996, Feng, Joseph and Huang 1996 and Hu 2001. A periodic array of spheres will be sucked together to form a long chain like that in figure V.3b. Prior to this computation the cause of chaining was in dispute; many persons thought that the mechanism responsible for chaining was shear thinning rather than the normal stresses which cause chaining in our simulations.

Cross stream migration and stable orientations of elliptic particles falling through an Oldroyd-B fluid in a two-dimensional channel were studied using the ALE particle mover. There are two critical numbers: the elasticity number and the velocity. For elasticity numbers below critical, the fluid is essentially Newtonian and the ellipse falls broadside-on down the channel centerline. For elasticity numbers larger than critical, the stable orientation depends on the the velocity: if the velocity is below the shear-wave speed, so that the viscoelastic Mach number is less than one, the ellipse falls down the channel centerline with its long axis parallel to the stream. For larger Mach numbers, the ellipse flips to the broadside-on orientation again, Huang, Hu and Joseph 1998. (An animation may be found in our Web site, *http://www.aem.umn.edu/Solid-Liquid_Flows*.)

## ▪ Sedimentation and Fluidization

Particle collision strategies may be put to a severe test in a sedimentation column. In the sedimentation problem, we start with a crystal of close-packed particles at the top of the column; then they settle under gravity resting in a crystal of close packed particles with defects on the bottom. The defect structure ought to be related to the collision strategies used, but this has not yet been tested. Fluidization is done in the same column. The particles first form a fixed bed at

the bottom; the inflow velocity is stepped up. First we find the so-called fluidizing velocity in which the fixed bed breaks up and the particles fluidize. The bed height is an increasing function of the inflow velocity; this gives the bed expansion by DNS. We have such a column in our laboratory; it is 3:2″ wide, 0:3″ deep and 20″ high. In simulations and experiments we use 0.25″ spheres so that the motion of the particles is confined basically to two dimensions though the fluid flow is in 3-D.

The fluidization in water of 1204 particles in three dimensions has been designated as a benchmark problem for DLM particle movers in parallel implementation. The simulations and experiments are discussed in Section VII. Animations of sedimentation and fluidization can be found on our web page.

## ▪ Mechanisms of Cross-Stream Migration

One of the uniquely useful features of DNS as compared with experiments is the ability to isolate effects. Typically in a real viscoelastic fluid the effects of viscosity, shear thinning and elasticity are all present. In simulations we may examine these effects one at a time: Newtonian, generalized Newtonian (shear thinning), Oldroyd-B, and Oldroyd-B with shear thinning. Results of 2-D simulation of 56 circular particles in a pressure driven spatially periodic channel flow, computed with the ALE particle mover are shown in figure V.5, Huang and Joseph 2000. The velocity profiles with and without particles are shown for each of the four cases. The difference between these two velocity profiles can be attributed to an effective two-fluid effect in which the particle-laden flow is regarded as an effective fluid with a higher effective viscosity. This higher viscosity is partly due to a slip velocity in particles lag the fluid, holding the fluid back. The slip velocity is the difference at a point between the average fluid and the average particle velocity there.

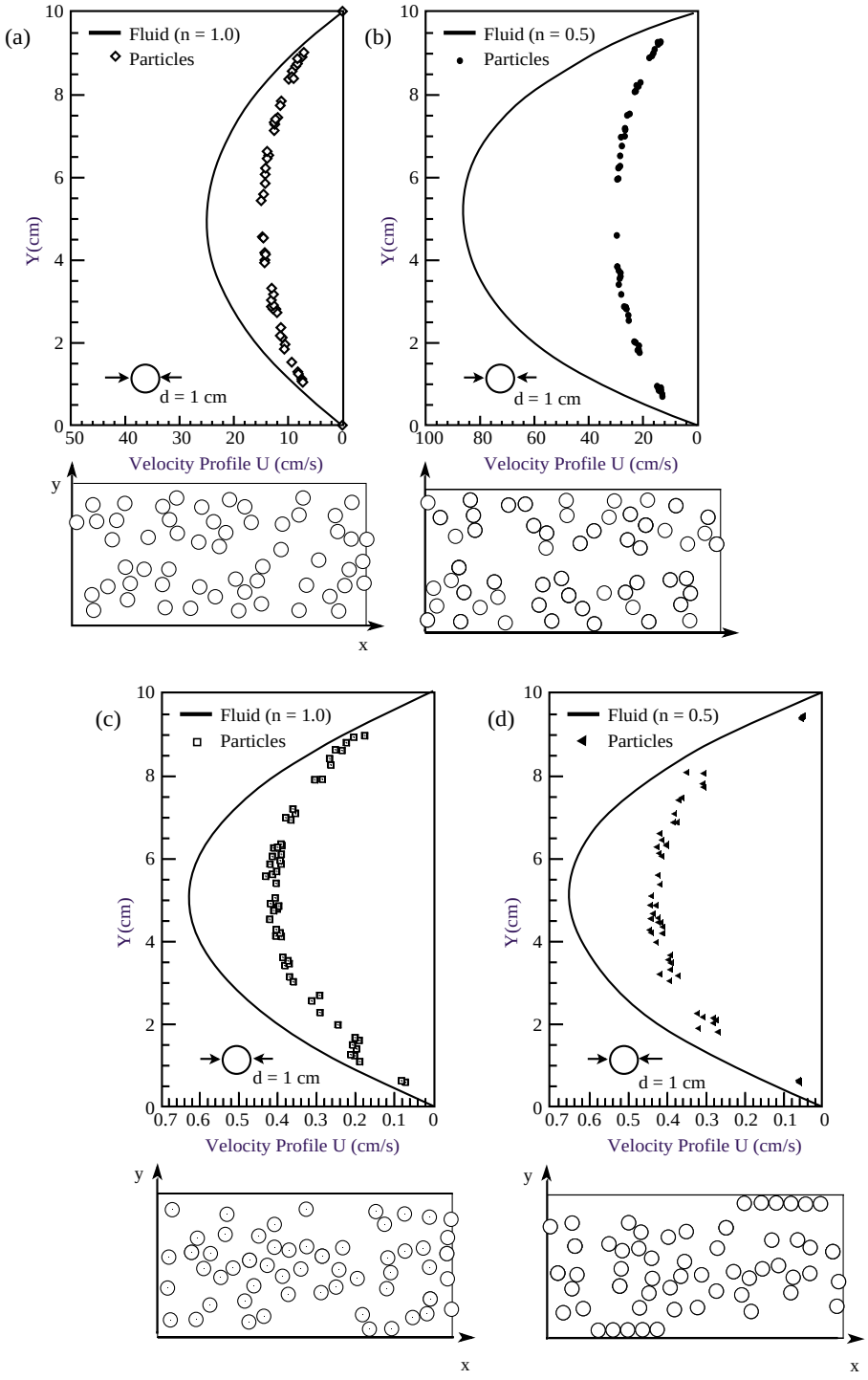


*Figure V.5: Cross stream migration of 56 neutrally buoyant circular particles in simulations of particle-laden Poiseuille flow using the ALE particle mover. The velocity profiles without and with particles are shown at the top of each sub-figure; underneath is a snapshot of the particle distribution. n is a power law index. (a) Newtonian fluid. The particles remain well dispersed, but a lubrication layer is evident. (b) Generalized Newtonian fluid. The particles migrate away from the center when the fluid is shear thinning. (c) Viscoelastic fluid (Oldroyd-B). The particles migrate toward the center with no shear thinning. (d) Viscoelastic fluid (Oldroyd-B). A clear annulus of fluid develops in the flow of an Oldroyd-B fluid with shear thinning (n = 0.5).*

## ▪ Slot Problems for Particle Transport in Fractured Reservoirs

We are going to focus on the problem of proppant transport in hydraulic fracturing applications. All of the features of slurry transport occur in hydraulic fracturing except that transport under turbulent conditions is not common. To understand proppant transport it is necessary to understand sedimentation, fluidization, particle migration and lubrication, lift-off and resuspension, slip coefficients, and strategies for handling contacting bodies.

Hydraulic fracturing is a process often used to increase the productivity of a hydrocarbon well. A slurry of sand in a highly viscous, usually elastic, fluid is pumped into the well to be stimulated, at sufficient pressure to exceed the horizontal stresses in the rock at reservoir depth. This opens a vertical fracture, some hundreds of feet long, tens of feet high, and perhaps an inch in width, penetrating from the well bore far into the pay zone. When the pumping pressure is removed, the sand acts to prop the fracture open. Productivity is enhanced because the sand-filled fracture offers a higher-conductivity path for fluids to enter the well than through the bulk reservoir rock, and because the area of contact for flow out from the productive formation is increased. It follows that a successful stimulation job requires that there be a continuous sand-filled path from great distances in the reservoir to the well, and that the sand is placed within productive, rather than non-productive, formations.

Under the flow conditions expected within the fracture during pumping, the sand particles migrate rapidly towards the center plane of the fracture, leaving a clear fluid layer at the fracture walls, Karnis and Mason 1966, Nolte 1988a, Tehrani, Hammond and Unwin 1994. This clear layer lubricates the motion of the slurry, and so increases the rate of gravity driven settling and density currents. The net result of these processes is to cause sand to accumulate at the bottom of the fracture and good vertical filling to be lost, Unwin and Hammond 1995. This in turn reduces well productivity and can also interfere with the fracture growth process by blocking downward extension.

The phenomenon of proppant migration is not currently controlled or exploited in the fracturing industry because the relationship between migration and fluid properties is not understood. DNS can give us this under standing (see figure V.5). The comparison of simulations with experiments is essential when the suspending fluid is viscoelastic because the constitutive equation for the fluid used in the experiments is never known exactly; it may be adequate for some flows and not for others. This is to be contrasted with the situation for Newtonian fluids, where a single constitutive equation applies in all the usual situations. It is therefore *extremely* important to develop particle movers for the viscoelastic fluids which are actually used in the fracturing industry and in other applications.

A typical vertical crack may be 3 meters high, 30 meters long and 2 cm wide. The diameter of a typical sand grain is 2 mm, so that the width-diameter ratio $h(x, y, t)/d$ is about 10. The sand density is 2.4. Because of geological features related to the overburden, the preferred crack orientation is vertical. Moreover, the dimensions of the fracture are not known a priori since the crack opens and shuts in response to local changes of pressure; fracture dynamics determining the slot dimensions is coupled to proppant transport.

In a slot problem a particle laden (say 20% solids) fluid is driven by a pressure gradient and the particles settle to the bottom as they are dragged forward. Sand deposits on the bottom of the slot; a mound of sand develops and grows until the gap between the top of the slot and the

mound of sand reaches an equilibrium value; this value is associated with a critical velocity. The velocity in the gap between the mound and the top of the slot increases as the gap above the mound decreases. For velocities below critical the mound gets higher and spreads laterally; for larger velocities sand will be washed out until the equilibrium height and velocity are reestablished, Kern *et al* 1959 (see figure V.6). The physical processes mentioned here are *settling* and *washout*. Washout could be by sliding and slipping; however, a more efficient transport mechanism is by *advection after suspension* which we studied by direct simulation.

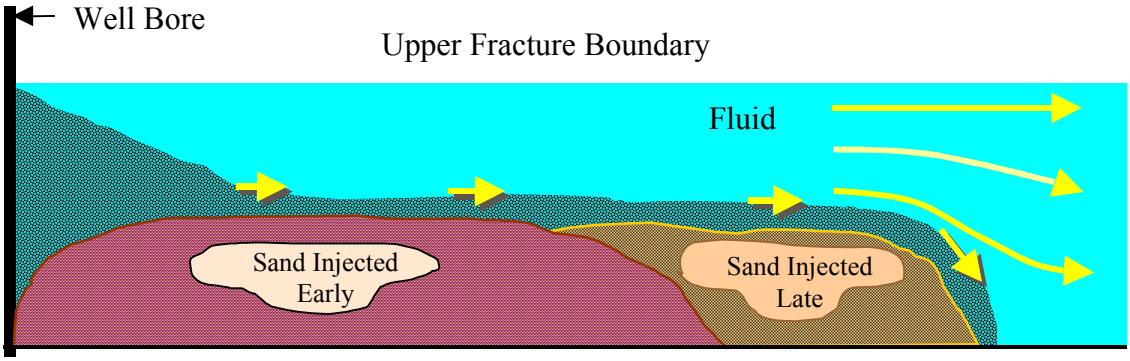


*Figure V.6 Sand transport in a fractured reservoir.*

## ▪ Lift-off, Resuspension, Equilibrium Height, Slip Velocities, Lift-Force Ratios

Using the ALE particle mover, we did *lift-off* and *slip-velocity* resuspension studies in Newtonian and viscoelastic fluids. A heavier particle is resting on the bottom of a channel in the presence of a shear (Poiseuille) flow at a certain critical speed. Depending on the weight and diameter of the particle, the fluid properties, and the aspect ratio of the channel, the particle rises from the wall to an equilibrium height at which the buoyant weight just balances the upward thrust of fluid forces. We found that the upward thrust (lift) is due to inertia; over 70% of the thrust is due to pressure. At equilibrium we compute the difference between the forward velocity and angular velocity of the particle and these same velocities in the fluid (at the center of the particle) when no particles are present. This gives the *slip velocity* and *angular slip velocity* which are needed for Richardson-Zaki 1954 type of correlations discussed in Section 4.3.

The problem of inertial lift on a moving sphere in contact with a plane wall in shear flow has been analyzed as a perturbation of Stokes flow with inertia in Cherukat and McLaughlin 1994, Krishnan and Leighton 1995, Leighton and Acrivos 1985. These studies lead to specific and useful analytic results expressed in terms of translational and rotational velocity and shear rate. The lift on a stationary sphere on a wall in a shear flow varies as the fourth power of the radius and the square of the shear rate. If the shear Reynolds number is sufficiently large, the lift force exceeds the gravitational force and the sphere separates from the wall.

The Stokes flow analysis is not valid for lift off of proppants; for these heavy particles our numerical results show lift off at shear Reynolds numbers in the hundreds. The perturbation analysis are of considerable value because they are analytic and explicit even though they are only valid well below the values characteristic of our applications.

# VI Modeling and DNS

One aim of direct numerical simulation (DNS) of solid-liquid flow is to guide the construction of models and to generate correlations which in days gone by were always generated by experiment. The single feature of such models is that the force that the fluid exerts on the particles is modeled rather than computed as it is in DNS. There are two types of models:

(1) Mixture (two-fluid) theories which are generated by averaging or by ad hoc procedures. These theories give rise to continuum theories in which the fluid phase and solid phase are defined at the same point; they are widely used in industry. In the construction of such theories interaction terms arise and their form is unknown. This is where the modeling comes in.

(2) Lagrangian numerical simulation (LNS). The fluid motion is resolved by DNS but the particles are moved by modeled forces as in mixture theory and are not computed.

## ▪ Averaging

In the past modeling was the main theoretical approach to solid-liquid flows. More recently high speed computers and improved software have made possible the development of direct numerical simulation of solid-liquid flow which can be used to validate models, to suggest new models and in some situations to replace models. It is necessary to develop techniques to interrogate direct simulation for useful descriptions, including those which impact modeling. It is almost always the case that model equations are field equations defined at each space-time (x,t) point. These equations give rise to the notion of interpenetrating continua in which actual material points are no longer identifiable, the solid and liquid phases are both present at each and every material point. The equations for such interpenetrating continua can be generated by averaging. Averaged equations generate averaged variables but the resulting equations are not simpler than the original equations from which they were derived. The averaging process generated more variables, averages of products, etc. than the number of equations; it is necessary to close the systems of equations and it is not possible for closure to apply to all flow. An extensive literature has grown up around the process of averaging the equations of motion, Anderson & Jackson 1967, Whitaker 1969, Wallis 1969, Delhaye 1969, Drew 1971, Drew & Segel 1971, Hinch 1977, Nigmatulin 1979, Drew 1983, Arnold, Drew & Lahey 1989, Joseph & Lundgren 1990, Wallis 1991, Drew & Lahey 1993, Zhang & Prosperetti 1994, 1997, Jackson 1997 and Drew and Passman 1999. Some authors have used local spatial averages taken over regions small in extent compared to macroscopic length scales of interest, others have averaged at each point of space over an ensemble of ‘macroscopically equivalent’ systems. Multiphase turbulent models have been discussed by Roco & Balakrishnam 1985 and by Roco 1990; these models give rise to predictions of the difference between the particle phase velocity and the composite velocity (slip velocity) for a five phase mixture.

The averaged equations of motions introduce interaction terms between the solids and fluid which and these terms must be modeled. The modeling of interaction terms in the averaged equations of motion is a form of guided and intelligent guessing. This modeling rather than the formal process of averaging is where the difficult part of the subject lies and compromises with mathematical rigor are inevitable.

It is at first glance curious that a “two-fluid” model arises from averaging solid-liquid flows. We have here continuum equations for the averages of the fluid, the fluid phase equations, and

for averages over the solid, solid phase equations. The generation of such equations by ensemble averaging is particularly transparent. Ensemble averages have the added advantage that they can be formally related to discrete time averages which are readily generated by direct simulation on fixed grids.

To generate ensemble averaged "two-fluid" equations we follow Joseph and Lundgren 1990.

We define an indicator function

$$H(\mathbf{x}) = \begin{cases} 0 & \text{if } \mathbf{x} \text{ is in the solid} \\ 1 & \text{if } \mathbf{x} \text{ is in the fluid} \end{cases} \tag{VI.1}$$

and let < > designate the operation of taking the average. The average is over many identical trials. We think of an experiment which is started at a certain time. At a later time and at a certain place, we record the value of some flow variable. We repeat the experiment, wait the same time, look at the same place and record again. After many trials we average the values by summing and dividing by the number $N$ of trials, then we let $N \to \infty$. In this manner, we generate a function $< >(\mathbf{x}, t)$. Now we get some identities using ensemble averaging and the indicator function. First

$$<H> = \varepsilon(\mathbf{x}, t) = 1 - \phi(\mathbf{x}, t)$$

is the fluids fraction and

$$<1 - H> = 1 - <H> = \phi(\mathbf{x}, t)$$

is the solids fraction. Recall that $\mathbf{V}(\mathbf{x}, t)$ is the true velocity. We define an average fluid velocity

$$\mathbf{V}_f(\mathbf{x}, t) = \frac{<H\mathbf{V}>}{<H>} = \frac{<H\mathbf{V}>}{\varepsilon} \tag{VI.2}$$

and an average solid velocity

$$\mathbf{V}_s(\mathbf{x}, t) = \frac{<(1-H)\mathbf{V}>}{<(1-H)>} = \frac{<(1-H)\mathbf{V}>}{\phi} \tag{VI.3}$$

The composite velocity is

$$\mathbf{V}_c(\mathbf{x}, t) = <\mathbf{V}> = <H\mathbf{V}> + <(1-H)\mathbf{V}> = \varepsilon \mathbf{V}_f + \phi \mathbf{V}_s \tag{VI.4}$$

We may define composite averages and mass averages of any quantity $f$ by

$$f_c = <f> = \varepsilon f_f + \phi f_s ,$$

$$f_m = \frac{<\rho f>}{<\rho>} = \frac{(\rho f)_c}{\varepsilon \rho_f + \phi \rho_s} ,$$

In particular the mass averaged velocity is

$$\mathbf{V}_m = \frac{<\rho\mathbf{V}>}{<\rho>} = \frac{\rho_f \mathbf{V}_f \varepsilon + \rho_s \mathbf{V}_s \phi}{\varepsilon \rho_f + \phi \rho_s} \tag{VI.5}$$

We next note $H(x,t)$ is a material variable for materials which do not change phase, always one following fluid particles, always zero following solids; i.e.

$$\frac{\partial H}{\partial t} + \mathbf{V} \bullet \nabla H = 0 \tag{VI.6}$$

Using this, and div $\mathbf{V} = 0$, we find

$$0 = <\frac{\partial H}{\partial t} + \mathbf{V} \bullet \nabla H> = <\frac{\partial H}{\partial t} + \text{div } H\mathbf{V}>$$

$$= \frac{\partial <H>}{\partial t} + \text{div } <H\mathbf{V}>$$

$$= \frac{\partial \varepsilon}{\partial t} + \text{div } \varepsilon \mathbf{V}_f \, . \tag{VI.7}$$

In the same way, we may show that

$$\frac{\partial \phi}{\partial t} + \text{div } \phi \mathbf{V}_s = 0 \, . \tag{VI.8}$$

It follows that

$$\text{div } \mathbf{V}_c = 0 \, . \tag{VI.9}$$

The reader can prove that

$$\frac{\partial \rho_c}{\partial t} + \text{div } (\rho_c \, \mathbf{V}_m) = 0 \, . \tag{VI.10}$$

We turn next to the momentum equations. Since

$$\frac{\partial H}{\partial t} + (\mathbf{V} \bullet \nabla) \, H = 0 \;\text{ and }\; \text{div } \mathbf{V} = 0 \tag{VI.11}$$

we have the identity

$$H \left( \frac{\partial \mathbf{V}}{\partial t} + [\mathbf{V} \bullet \nabla] \mathbf{V} \right) = \frac{\partial H\mathbf{V}}{\partial t} + \text{div } H \, \mathbf{VV} \, . \tag{VI.12}$$

The momentum equation for the fluid and the solid is

$$\rho \left( \frac{\partial \mathbf{V}}{\partial t} + [\mathbf{V} \bullet \nabla] \mathbf{V} \right) = \text{div } \mathbf{T^*} + \rho \mathbf{b} \, . \tag{VI.13}$$

Multiply (VI.13) by $H$ and ensemble average, using (VI.6),

$$\rho_f \frac{\partial}{\partial \text{t}} <H\mathbf{V}> + \rho_f \, \text{div } <H \, \mathbf{VV}> = <H \, \text{div } \mathbf{T^*}> + \rho_f \, \mathbf{b}_f \, \varepsilon \, . \tag{VI.14}$$

Now we differentiate by parts

$$<H \text{ div } \mathbf{T}^*> = \text{div } <H\mathbf{T}^*> - <\nabla H \bullet \mathbf{T}^*> \tag{VI.15}$$

where

$$\nabla H = \delta_\Sigma(\mathbf{x})\, \mathbf{n}\ ,\ \nabla <H> = <\nabla H> = <\delta_\Sigma \mathbf{n}> = \nabla \varepsilon\,(\mathbf{x}, t)\ , \tag{VI.16}$$

and $\delta_\Sigma\,(\mathbf{x})$ is a one-dimensional Dirac's delta function across the solid-fluid interface, $\mathbf{n}$ is the outward normal to the solid. We next note that $\mathbf{n} \bullet \mathbf{T}^* = \mathbf{t}$ is the traction vector at a point $\mathbf{x}_\Sigma$ on the interface. From the definitions of $\mathbf{T}_f^*$ we have

$$<H\mathbf{T}^*> = \varepsilon\, \mathbf{T}_f^*\ (\mathbf{x}, t) \tag{VI.17}$$

Using these relations, we may write (VI.14) as

$$\rho_f \left[ \frac{\partial}{\partial t}\ \varepsilon \mathbf{V}_f + \text{div } <H\mathbf{V}\mathbf{V}> \right] = \text{div } \varepsilon \mathbf{T}_f^* - <\delta_\Sigma\,(\mathbf{x})\mathbf{t}> + \rho_f\, \varepsilon\, \mathbf{b}_f\ . \tag{VI.18}$$

Using the same method, we find a momentum equation for the solid in the form

$$\rho_s \left( \frac{\partial \phi \mathbf{V}_s}{\partial t} + \text{div } <(1-H)\mathbf{V}\mathbf{V}> \right) = \text{div } \phi\, \mathbf{T}_s^* + <\delta_\Sigma\,(\mathbf{x})\mathbf{t}>\ + \rho_s\, \phi\, \mathbf{b}_s\ . \tag{VI.19}$$

Let us assume now that the fluid phase is Newtonian,

$$\mathbf{T}^* = -p\mathbf{1} + 2\,\eta\, \mathbf{D}\ [\mathbf{V}]\ \text{ in the fluid,} \tag{VI.20}$$

and the solid phase is a rigid body for which

$$\mathbf{D}\ [\mathbf{V}] = 0 \text{ on solids,} \tag{VI.21}$$

where

$$\mathbf{D}\ [\mathbf{V}] = \frac{1}{2}\ \ (\nabla \mathbf{V} + [\nabla \mathbf{V}]^T) \tag{VI.22}$$

is the rate of strain. The stress for the fluid phase is given by

$$\begin{aligned} \mathbf{T}_f = \varepsilon \mathbf{T}_f^* &= <H\mathbf{T}^*> = <H\,(-p\mathbf{1} + 2\,\eta\, \mathbf{D}\ [\mathbf{V}])> \\ &= -\varepsilon\, p_f\, \mathbf{1} + 2\,\eta\ <(H-1)\ \mathbf{D}\ [\mathbf{V}]> + 2\,\eta\ <\mathbf{D}\ [\mathbf{V}]> \\ &= -\varepsilon\, p_f\, \mathbf{1} + 2\,\eta\ \ \mathbf{D}\ [<\mathbf{V}>] \\ &= -\varepsilon\, p_f\, \mathbf{1} + 2\,\eta\ \ \mathbf{D}\ [\mathbf{V}_c] \end{aligned} \tag{VI.23}$$

where we have $<\mathbf{V}> = \mathbf{V}_c = \mathbf{v}_c$, and

$$<(H-1)\ \mathbf{D}\ [\mathbf{V}]> = 0 \tag{VI.24}$$

because $H$–1 is zero in the fluid and $\mathbf{D}[\mathbf{V}] = 0$ in the solid. The step $\langle \mathbf{D}[\mathbf{V}] \rangle = \mathbf{D}[\langle \mathbf{V} \rangle]$ is true because $\mathbf{V}$ is continuous, $\mathbf{D}[\mathbf{V}]$ is uniformly bounded. In the modeling of multiphase flows of rigid particles, it is convenient to write

$$\mathbf{T}^* = -p\mathbf{1} + \boldsymbol{\tau} \tag{VI.25}$$

where p is the mean normal stress. The ensemble average of this is

$$\mathbf{T}_S = \phi\, \mathbf{T}_S^* = -\phi\, p_S\, \mathbf{1} + \langle (1-H)\boldsymbol{\tau} \rangle \tag{VI.26}$$

where

$$\phi\, p_S = \langle (1 - H)\, p \rangle\,. \tag{VI.27}$$

The expression (VI.26) with $\tau = 0$ is frequently postulated in mixture theories (e.g., Nunziato, Passman, Givler, MacTigire and Brady 1986). Givler 1987 argues that $p_S$ may be interpreted as the average of the local pressure field around an isolated particle. Our DLM formulation following (VI.19) suggests that $p = 0$. If we assume (VI.23), (VI.24), and (VI.26), and manipulate the inertia terms to a more elegant form, we get the following system of ensemble averaged equations.

$$\frac{\partial \varepsilon}{\partial t} + \text{div}\ \varepsilon\, \mathbf{v}_f = 0\,, \tag{VI.28}$$

$$\frac{\partial \phi}{\partial t} + \text{div}\ \phi\, \mathbf{v}_S = 0\,, \tag{VI.29}$$

$$\rho_f\, \varepsilon \left( \frac{\partial \mathbf{v}_f}{\partial t} + \mathbf{v}_f \bullet \nabla \mathbf{v}_f \right) + \rho_f\, \text{div} \langle H\, (\mathbf{V} - \mathbf{v}_f)\, (\mathbf{V} - \mathbf{v}_f) \rangle$$
$$= -\nabla\, (\varepsilon p_f) + \eta\, \nabla^2 \mathbf{v}_c - \langle \delta_\Sigma(\mathbf{x})\, \mathbf{t} \rangle + \varepsilon\, \rho_f\, \mathbf{b}_f\,, \tag{VI.30}$$

$$\rho_S\, \phi \left( \frac{\partial \mathbf{v}_S}{\partial t} + \mathbf{v}_S \bullet \nabla \mathbf{v}_S \right) + \rho_S\, \text{div} \langle (1-H)\, (\mathbf{V} - \mathbf{v}_S)\, (\mathbf{V} - \mathbf{v}_S) \rangle$$
$$= -\nabla\, (\phi\, p_S) + \langle \delta_\Sigma(\mathbf{x})\, \mathbf{t} \rangle + \text{div} \langle (1-H)\, \boldsymbol{\tau} \rangle + \phi\, \rho_S\, \mathbf{b}_S\,. \tag{VI.31}$$

The boundary conditions between the fluid and the particle takes form in the traction vector term in (VI.30) and (VI.31). The addition of a constant pressure to the system as a whole, to $p_f$, $p_S$ and $\mathbf{t}$ simultaneously, has no dynamic consequence. The proof of this uses (VI.16) and it works even if $p_s = 0$.

When we add (VI.28) and (VI.29), we get

$$\text{div}\ \mathbf{v}_c = 0\,.$$

When we add (VI.30) and (VI.31) we get an equation for the total momentum in which the mutual forces (the traction vector) vanishes as it does in the weak solution formulation for DNS (chapter II).

The existence of two fluid equations even when one of the fluids is solid is perfectly justified by ensemble averaging. These equations, like other two fluid models, are not closed and methods

of closure, or constitutive models for the interaction terms, are required to put the equations into a form suitable for applications. Moreover, since averaging over repeated identical trials is not a realizable proposition, the ensemble averaged variables are conceptually abstract and their relation to more physically intuitive variables, like the ones which arise from spatial averaging, is uncertain.

There are two kinds of two-fluid models of solid-liquid flow; one (more difficult) requires the modeling of forces on the particles and a second in which the particle-laden portions of the fluid are regarded as another fluid with different fluid properties, like an effective density and viscosity. The first kind of theory can be framed as ensemble averaged equations, those just given, in which there are more unknowns than equations. These equations must be closed by modeling unknown terms; this modeling is difficult and can never cover all possible situations; it is better to compute the forces. The second, effective theory is obviously a rather severe form of modeling but it can work well in restricted problems as in the sedimentation of 6400 circles studies in chapter VIII.

There are many problems of mechanics in which averaging of any kind is inappropriate, leading to correct but irrelevant statements, like "the average weather is widely scattered showers" or "the average gender is slightly female."

## ▪ Fluidization by Drag and Fluidization by Lift

We are going to develop procedures for converting data from DNS to models for problems of fluidization. Two kinds of problems are under consideration: fluidized beds in which the particles are fluidized by *drag forces* opposing gravity and slurry beds in pipes and conduits in which the flow is perpendicular to gravity and the particles are fluidized by *lift forces*.

Flows in which particles are suspended in a balance of drag and weight are fluidized suspensions. Flows in which particles are suspended by lift forces perpendicular to the motion of the fluid are fluidized by lift.

## ▪ Fluidization and Sedimentation

In a fluidized suspension, the particles are stationary on the average and the fluid moves up through them. It can be said that the particles are stationary under weight and drag. Fluidized beds are amazing because of the action of hindered setting; a single particle will be held stationary under a balance of weight and drag at one velocity and only one velocity. If the velocity is smaller, the particle will fall to the bottom of the bed and if the velocity is larger, the particle will be blown out of the bed. In the case of many particles, the situation is different; a unique velocity is not required for fluidization. After the particles are fluidized, an increase in the velocity will increase the height of the bed, the void fraction will increase, the center of mass of the suspension will rise. The opposite is true of when the velocity is decreased.

It is not possible to fluidize a bed of heavy particles at low velocities. The bed fluidizes all at once at the critical fluidization velocity; after this, the raising and lowering of the fluidizing velocity raises and lowers the center of gravity of the fluidized suspension.

The remarkable properties of fluidized suspensions are associated with a hindered settling function. Settling of a suspension at terminal velocity is like a fluidized bed in a coordinate

system moving with the fluidization velocity; in this system the particles fall. The hindered settling is controlled by the changes in the solid or void fraction. The velocity of the fluid through the particles is greater than the input velocity because the flow must go between the particles and the effective density and viscosity of the suspension is different than the viscosity and density of the fluid.

## ▪ Two Differences Between Fluidization and Sedimentation

The first difference is that in a fluidized bed you are driving the fluid even when there are no particles. Hence there is a shear stress at the wall of the bed even when there are no particles. In the case of sedimentation, there is no driving force when particles are absent, hence the wall stress is absent in this case apart from that due to the falling particles. Sedimentation and fluidization may be quite different when the wall effects are large.

A second difference is the contrary behavior of the top of a fluidized bed and the bottom of a sedimenting bed. The top of a fluidized top is flat, perpendicular to gravity, more or less. The less part can be seen when a particle is impelled out of the top by some hydrodynamic event; it will always fall back because the drag on the single particle is less than the drag on the particles in suspension. "Out of flat" dynamics is unstable and a top for an expended bed is a robust feature of fluidization.

On the other hand, the bottom of a suspension of settling particles is always unstable because the particles that fall away from the bottom experience a decreased drag, and will not back into the suspension. At the bottom of the sedimenting bed you see the formation of fingers like those in Rayleigh-Taylor instability when heavy fluid is over light.

## ▪ Uniform Fluidization

By a state of uniform fluidization we mean a constant state in which time and space derivatives of averaged quantities vanish. In this case, we may assume that all the terms in equations (VI.30), (VI.31) vanish except the pressure gradient and the body force term. After adding (VI.30) and (VI.31) written as

$$p \overset{def}{=} p_c = \varepsilon p_f + \phi\, p_s, \mathbf{b} = -e_z g \tag{VI.32}$$

we get

$$\frac{\Delta p}{h} = \rho_s \phi \;\; g + \rho_f \varepsilon g \tag{VI.33}$$

and when $h = H_e$

$$\frac{p_1 - p_2}{H_e} = \rho_s \phi \;\; g + \rho_f \varepsilon g = \left(\rho_s \Omega_s + \rho_f \Omega_f\right) g/\Omega \tag{VI.34}$$

where, neglecting wall friction,

$$p_2 - p_a = \rho_f g\left(L - H_e\right) .$$

After noting that $\Omega = HA, \Omega_f = \Omega - \Omega_s$, we get

$$p_1 - p_2 = \rho_f g H_e + (\rho_s - \rho_f)\Omega_s / A \ . \tag{VI.35}$$

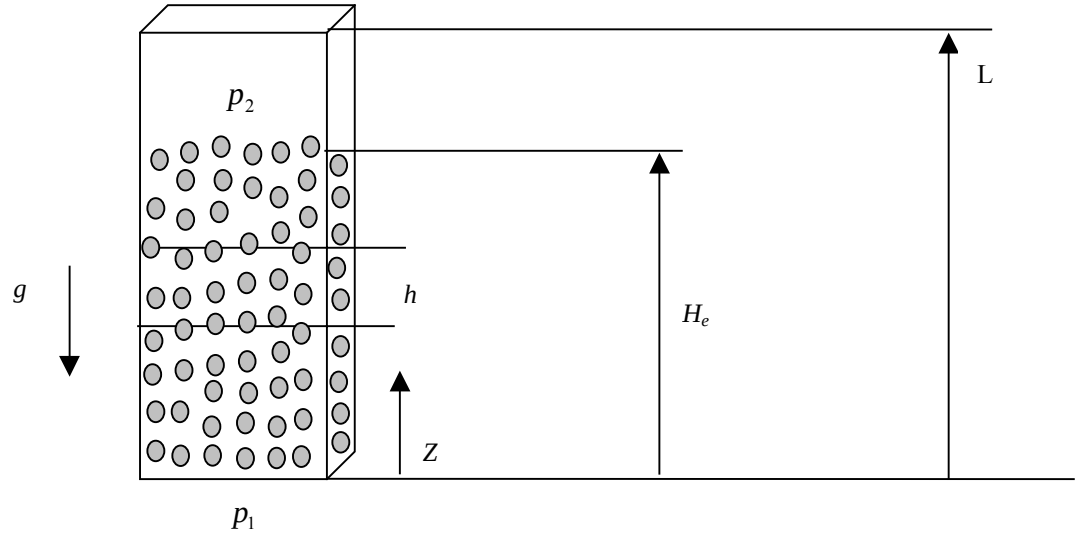


*Figure VI.1 Cartoon of a fluidized bed expanded to height* $H_e$. *The total volume under* $Z = H_e$ *is* $\Omega = H_e A$ *where* A *is the cross section of the bed;* p *is the pressure and* $p_a$ *is atmospheric pressure.*

Since the volume, $\Omega_s$ of solids under $H_e$ is fixed (given by $\Omega_s = \frac{4}{3}\pi a^3 N$ for $N$ uniform spheres of radius $a$ equation (VI.35) shows that the bed height $H_e$ is a linear function of the pressure difference; the bed height (or fluid fraction) increases with the applied pressure difference.

The pressure difference, $\Delta p$, between fixed stations $h$ apart given by (VI.33) must decrease because $(\rho_s - \rho_f)\ \phi - \rho_f$ will decrease with the solids fraction $\phi$ in an expanding bed.

## ▪ Incipient Fluidization

If the pressure difference across the bed is not great enough to lift the particles plus fluid, the particles will rest one on another in a fixed bed, a *porous media* satisfying Darcy's law. The height $H_c$ when the spheres are close packed is given by

$$\alpha = \Omega_s / H_c A \tag{VI.36}$$

where for a monosized dispersion of spheres $\alpha$ = 3/4. For incipient fluidization put $H_e = H_c$ in (VI.35), using (VI.36), to find that

$$A(p_1 - p_2)_c = g\Omega_s \{\rho_f \left(\frac{1}{\alpha} - 1\right) + \rho_s\} \tag{VI.37}$$

The force (VI.37) is just what we need to overcome the overburden of fluid plus solids.

Equation (VI.34) predicts what one expects to read as the pressure difference between transducers at $Z = 0$ and $Z = H_e$. An equivalent formulation can be based on the dynamic pressure gradient which is obtained from (VI.32) by splitting the total pressure

$$\frac{dp}{dz} = \left(\frac{dp}{dz}\right)_f + \rho_f g \tag{VI.38}$$

into a dynamic part and a part balancing the liquid head. This gives

$$\left(\frac{dp}{dz}\right)_f = \left[\rho_s \phi + \rho_f (\varepsilon - 1)\right] g = \left(\rho_s - \rho_f\right) \phi \; g \,. \tag{VI.39}$$

Richardson and Zaki 1954 note that the validity of (VI.39) was verified experimentally by Wilhelm and Kwauk 1948 and by Lewis, Gilliard and Bauer 1949; it has been used frequently up to this time but is valid only when the pressure drop due to the confining walls is negligible.

## ▪ Hindered Settling

In one-dimensional approximations of fluidized suspensions, the drag is balanced by the buoyant weight (VI.13). This is like pipe flows where the frictional pressure gradient is balanced against the drag of the shear stresses at the tube wall; here it is the drag against the particles that is reckoned to be most important.

Modeling of drag forces in one dimensional sedimenting or fluidizing suspensions is still a controversial subject; many models have been proposed and there is no consensus. Some of the more popular models are due to Barnea and Mizrachi 1973, Foscolo and Gibalaro 1984, 1987, Batchelor 1974 and others.

The drag models proposed so far require expressions for the hindered sedimentation of fluidization velocity of suspensions of particles. The composite velocity of a fluidized suspension of volume fraction $\phi$

$$V(\phi) = V_c = V_s \phi + V_f (1 - \phi) \tag{VI.40}$$

is the volume flux divided by the total area which is independent of Z, $\partial V_c / \partial Z = 0$, by (8), and hence is equal to the superficial inlet velocity. The velocity

$$V(0) = V_f$$

is the velocity required to fluidize a single sphere. $V(\phi)$ and $V(0)$ are also sedimenting velocities for many and one single sphere, but here we shall carry out the analysis only for fluidization to avoid confusion. We also define

$f(\phi)$ drag on a sphere in a suspension of volume fraction $\phi$,

$f(0)$ drag on a single sphere $\phi = 0, \varepsilon = 1$,

$F(0) = 6\phi \, f(\phi) / \pi d^3$ drag per unit volume.

To explain the factors which lead to hindered settling we can consider the special case described by Stokes flow. All of the above quantities depend on the Reynolds number *R*.

$$R = \frac{V(0) d \rho_f}{\eta_f}.$$

For the Stokes flow $R \to 0$ and $[V_0(\phi), f_0(\phi)] = \lim_{R \to 0} [V(\phi, R), f(\phi, R)]$

In steady flow, the drag $f_0(0)$ balances the buoyant weight;

$$f_0(0) = 3\pi \eta_f d U_0(0) = \frac{\pi d^3}{6} (\rho_s - \rho_f)\, g \tag{VI.41}$$

where $\eta_f$ is the fluid viscosity.

To generalize (VI.41) for hindered settling effects we first note that there increase of velocity through the particles (back flow in a sedimenting suspension), as that the velocity past the particles is increased to

$$\widehat{V}_0 = V_0(\phi)/\varepsilon \ . \tag{VI.42}$$

The viscosity of the suspension is increased to

$$\eta(\phi) = \eta_f \theta(\phi) \tag{VI.43}$$

where $\theta(\phi) > \theta(0) = 1$ and the buoyant weight is reduced from the value on the left of (10) to

$$\pi d^3 (\rho_s - \rho_c)\ \ g/6 = \pi d^3 (\rho_s - \rho_f)\ \ \varepsilon\, g/6 = \varepsilon f_0(0). \tag{VI.44}$$

The replacement of $\rho_f$ by $\rho_c$ is controversial; different credible scholars have different opinions. The experiments of Poletto and Joseph 1995 support the replacement of $\rho_f$ with $\rho_c = \rho_s \phi + \rho_s (1 - \phi)$ as long as the sedimenting sphere is not too much larger than the spheres in the suspension.

Now rewrite the drag law (VI.41) replacing the viscosity $\eta_f$ with the effective viscosity (VI.43) and the fluid density with $\rho_c$ to get

$$f_0(\phi) = 3\pi d \eta_f \theta(\phi) \widehat{V}_0 = 3\pi d \eta_f \theta(\phi) V_0(\phi)/\varepsilon = \varepsilon f_0(0) = \varepsilon 3\pi d \eta_f V_0(0). \tag{VI.45}$$

From (VI.44) it follows that

$$V_0(\phi) = (1 - \phi)^2 V_0(0)/\theta(\phi) = h(\phi) V_0(0) \tag{VI.46}$$

where $h(\phi)$ is the hindered settling function.

Equation (VI.46) rests on many unproven assumptions; if valid, it is valid only for slow and only when wall effects are negligible. Barnea & Mizrachi 1973 give

$$h(\phi) = (1-\phi)^2 \big/ (1+\phi^{1/3}) \exp[5\phi/3(1-\phi)]$$

where the exponential represents effective viscosity and $\phi^{1/3}$ is used to represent the effect of walls by close packed spheres.

A very accurate expression for hindered settling, which is not restricted to Stokes flow and accounts for wall effects in cylindrical tubes of diameter $D$ was obtained from extensive experiments on the sedimentation and fluidization of monosized spheres by Richardson & Zaki 1954. They found that the composite fluidization velocity (or fall velocity of sedimenting suspension) is given by

$$V(\phi) = V(0)(1-\phi)^n \tag{VI.47}$$

where

$$n = 4.65 + 19.5 \, d/D \text{ when } R = V(0)\, d/\nu < 0.2\,,$$

$$n = (4.36 + 17.6 \, d/D) R^{-0.03} \text{ when } 0.2 < R < 1, \tag{VI.48}$$

$$n = 4.45 R^{-0.1} \text{ when } 1 < R < 500\,,$$

$$n = 2.39 \text{ when } 500 < R < 7000\,.$$

The terminal velocity $V(0)$ of an isolated sphere should also be retarded by the effect of nearby walls. One frequently used empirical formula

$$V_0(0) = \frac{(\rho_s - \rho_f) d^2}{18 \eta_f} \left(1 - \frac{d}{D}\right)^{2.25} \tag{VI.49}$$

valid for slow flow, is due to Francis 1933.

The Richardson & Zaki correlation (VI.47) shows that the largest fluidization velocity $V(0)$ is for a single sphere or the equivalent which is an infinitely expanded bed in which one sphere exerts no influence on another. When $V > V(0)$ the spheres are dragged out of the bed, blown away. In general $V(\phi)$ decreases as $\phi$ increases. The bed won't rise if $V > V(\phi_{MP})$ where $\phi_{MP}$ is the packing of a fixed bed and $V(\phi_{MP})$ is the incipient fluidization velocity. In an expanded bed

$$V(\phi_{MP}) \le V(\phi) \le V(0)\,.$$

The correlation (VI.47) and (VI.48) of Richardson & Zaki can be said to be the empirical foundation of many engineering theories of fluidization and sedimentation.

## ▪ Drag and Hindered Settling

The relation between the drag $f(\phi)$ and composite velocity $V(\phi)$ is obtained by generalizing the relation between the drag $f(0)$ and the velocity $V(0)$ for a single particle in an otherwise particle free fluid in much the same way that we carried out this correlation for Stokes flow. A popular empirical formula relating drag and velocity for a single particle is due to Dallavalle 1948,

$$C_D = \left( \frac{0.63 + 4.9}{\sqrt{R}} \right)^2 = \frac{8 f(0)}{\rho_f \pi d^2 V^2(0)} \tag{VI.50}$$

where

$$R = \frac{V(0) d}{\nu} \tag{VI.51}$$

and

$$f(0) = \frac{\pi d^3}{6} \left( \rho_s - \rho_f \right) g \tag{VI.52}$$

balances the buoyant weight. Replacing $\rho_f$ with $\rho_c(\phi)$ for the suspension, we find that

$$f(\phi) = \varepsilon f(0) = \frac{\varepsilon}{8} \rho_f \pi d^2 V^2(0) \left( 0.63 + 4.9 \sqrt{\frac{\eta_f}{\rho_f V(0) d}} \right)^2 . \tag{VI.53}$$

After replacing $V(0) = V(\phi)/(1-\phi)^n$ from (VI.47), putting $V(\phi) = V_c$ from (VI.40), (VI.53) becomes

$$f(\phi) = \frac{\rho_f}{8} \pi d^2 \frac{V_c^2}{(1 - V_c^2 \phi)^{2n-1}} \left( 0.63 + 4.9 \sqrt{\frac{\eta_f (1-\phi)^n}{\rho_f V_c d}} \right)^2 . \tag{VI.54}$$

An important step the Richardson-Zaki correlation (VI.48) is all important. Expanding (VI.54), we find, using *n* in (VI.48), that

$$f(\phi) = \begin{cases} 3.3 \pi d \eta_f V_c (1-\phi)^{-3.78} & \text{small } R, \\ 0.0463 \pi \rho_f d^2 V_c{}^2 (1-\phi)^{-3.65} & \text{large } R, \end{cases} \tag{VI.55}$$

Foscolo, Gibilaro and Waldman 1983 note that if we replace 2.39 with 2.4 and 4.65 with 4.8 in (VI.48) and 4.9 in (VI.54) with 4.8, then

$$f(\phi) = \varepsilon^{-3.8} \begin{cases} 3 \pi d \eta_f V_c & \text{laminar}, \\ 0.0463 \pi \rho_f d^2 V_c{}^2 & \text{turbulent}, \end{cases} \tag{VI.56}$$

Evaluating (VI.56) for $\phi = 0(\varepsilon - 1)$ we have

$$f(0) = \begin{cases} 3\pi d\eta_f V(0) \\ 0.0463\pi\rho_f d^2 V^2(0) \end{cases}. \tag{VI.57}$$

Since $\varepsilon = \left(V(0)/V_c\right)^{1/n}$ from (VI.47)

$$\varepsilon^{4.8} = \left[\frac{V(0)}{V_c}\right]^{4.8/n}. \tag{VI.58}$$

Obviously

$$\left[\frac{V_c}{V(0)}\right]^{\frac{4.8}{n}} = \begin{cases} V_c/V(0) & \text{when } n = 4.8 \\ V_c^2/V^2(0) & \text{when } n = 2.4. \end{cases} \tag{VI.59}$$

Hence, using (VI.57) and (VI.59), we find that

$$\left[\frac{V_c}{V(0)}\right]^{\frac{4.8}{n}} f(0) = \begin{cases} 3\pi\eta_f V_c & \text{when } n = 4.8 \\ 0.0463\pi\rho_f d^2 V_c^2 & \text{when } n = 2.4 \end{cases} \tag{VI.60}$$

and

$$f(\phi) = \varepsilon^{-3.8}\left[\frac{V_c}{V(0)}\right]^{\frac{4.8}{n}} f(0) \tag{VI.61}$$

where $n$ is the Richardson-Zaki exponent with 2.4 replacing 2.39 and 4.8 replacing 4.65, $f(0)$ and $V(0)$ are related by the Dallavalle formula (VI.50) with 4.8 replacing 4.9.

$f(\phi)$ is a drag law which satisfies (VI.53); that is, $f(\phi) = \varepsilon f(0)$ which must hold when the drag is balanced by the buoyant based on $\rho_c$, and correctly reduces to (VI.56) for small and large Reynolds numbers.

The drag law (VI.61) relies heavily on empirical data for "steady flow." Dallavalle's expression is an empirical formula to fit experimental data for steady flow over a sphere and the Richardson-Zaki correlation is for "steady" fluidization which certainly is steady only in a statistical sense whose main consequence is that the average particle velocity $V_s = 0$ and $V_c = \varepsilon V_f$. The reliance on good empirical correlations in making two-fluid models of solid-liquid flow is to be commended. Approaches in this subject which purport to be from first principles usually miss the mark; they are rigorous but remain at a level too general for practical results or they give practical results only after making assumptions which are not rigorous. The excellence of such theories ought to be validated by how well they correspond to what is known for sure. For this validation direct simulation is a useful tool.

## ▪ Dynamic and One Dimensional Models

Foscolo and Gibilaro 1984 developed a one-dimensional model for the analysis of the stability of fluidized beds. Batchelor 1988 developed a similar theory; he gave different plausibility arguments to justify the terms, one-by-one in his equations. Both authors present a one-dimensional equation for the particle phase; nothing whatever is said about the fluid phase. This procedure is equivalent to a form of "pre-closure", since the fluid phase is neglected, the constraint $\partial V_c/\partial Z = 0$ coming from (VI.9) is lost. In this case the composite pressure (or $p_s$) cannot be considered to be an unknown in the dynamical system for incompressible constituents, but must be modeled as an "equation of state" associated with a compressible solids fraction satisfying

$$\frac{\partial \phi}{\partial t} + \frac{\partial \phi V_s}{\partial Z} = 0 . \tag{VI.62}$$

The momentum equation of Foscolo and Gibilaro 1984 is presented in the form

$$\phi \rho_s \left( \frac{\partial V_s}{\partial t} + V_s \frac{\partial V_s}{\partial Z} \right) = F + \frac{\partial \pi_s}{\partial Z} \tag{VI.63}$$

where $\pi_s = p_s - P$ is the dynamic part of $p_s$ (due to motion) and $\partial P/\partial Z = -\phi \rho_s g$ balances the weight of the particles. To close this system Foscolo and Gibilaro model the two terms on the right side of (VI.63). They argue that

$$\pi_s = -\frac{2}{3} dF \tag{VI.64}$$

and construct $F$ from (VI.61) using the following plausibility argument. A particle will be dragged up if

$$V_c - V_s = \varepsilon (V_f - V_s) > 0 . \tag{VI.65}$$

In solid liquid models slip velocities may be defined in different ways; $V_f - V_s$ is often called a slip velocity but $V_c - V_s$ can also be called a slip velocity which reduces properly to $V_c$ for steady flow, when $V_s = 0$. Foscolo and Gibilaro 1984 introduce and unsteady drag force

$$f(\phi) = \varepsilon^{-3.8} \left[ \frac{V_c - V_s}{V(0)} \right]^{\frac{4.8}{n}} f(0) \tag{VI.66}$$

such that $f(\phi) = f(0)$ when. $V_s = 0$ In unsteady flow the force $F$ on a single sphere is the unsteady drag $f(\phi)$ minus the buoyant weight given by (VI.44). After replacing $f(0)$ with (VI.52) they get

$$\Im = \frac{\pi d^3}{6}(\rho_s - \rho_f)g\left(\left[\frac{V_c - V_s}{V(0)}\right]^{\frac{4.8}{n}} \varepsilon^{-3.8} - \varepsilon\right). \tag{VI.67}$$

The unsteady force $F(\phi)$ per unit volume is $N\Im/\Omega$, where $N$ is the number of spheres in the volume $\Omega = \Omega_s/\phi$ where $\phi = \Omega_s/\Omega$ and $\Omega_s = N\pi d^3/6$. Hence

$$F = \phi(\rho_s - \rho_f)g\left(\left[\frac{V_c - V_s}{V(0)}\right]^{\frac{4.8}{n}} \varepsilon^{-3.8} - \varepsilon\right). \tag{VI.68}$$

Foscolo and Gibilaro 1984 argue that the same forces of the fluid on the particles acts at the boundary to keep the particles from dispersing; to get this force we need to multiply the force per unit volume by the ratio $2d/3$ of the volume to the surface area of the sphere leading to (VI.67).

## ▪ Particle Phase Pressure and the Stability of Uniform Fluidization

There is ever so much talk about the particle phase pressure. It boggles the mind to know how such a quantity might be defined on a rigid body (of equation V.20). The choice of the expression for the particle phase pressure in one-dimensional one-phase Foscolo and Gibilaro 1984, Batchelor 1988 and two-phase models Wallis 1969 determines whether or not the constant state $V_s = 0$ and $\varepsilon = \varepsilon_0$ is stable. In a pioneering work Wallis 1969 derives a linear equation for the perturbation $\varepsilon'$ of $\varepsilon_0$ which he puts into the form

$$\frac{\partial\ \varepsilon'}{\partial t^2} + 2V_0\frac{\partial^2\varepsilon'}{\partial Z\partial t} + A\frac{\partial^2\varepsilon'}{\partial Z^2} + B\left(\frac{\partial\varepsilon'}{\partial t} + V_\omega\frac{\partial\varepsilon'}{\partial Z}\right) = 0. \tag{VI.69}$$

This is a hyperbolic equation with forward and backward "elastic" waves associated with 2nd order terms and a continuity wave associated with the first order terms. Instability occurs when the square of the speed of the continuity wave is greater than the square of the speed of the elastic wave. However, the coefficients in the Wallis equations are not precisely given as they are in theories of Foscolo and Gibilaro 1984 and Batchelor 1988. Foscolo and Gibilaro argue that

$$\frac{\partial F}{\partial Z} = \frac{N}{\Omega}\frac{\partial\Im}{\partial\varepsilon}\frac{\partial\varepsilon}{\partial Z} \tag{VI.70}$$

and they derive a criterion for the stability of the uniform state which they show agrees reasonably well with observations of the formation of particle free three-dimensional regions which resemble bubbles rising through liquids. Of course, strictly speaking a three-dimensional disturbance cannot be described by a one-dimensional equation.

Batchelor 1988 does not argue his theory in the same way as Foscolo and Gibilaro 1984. He does not believe in two-fluid models and argues out the terms of his equations by physical reasoning. The term in his equation corresponding to the particle phase pressure is regarded by him as arising from the diffusion of particles as in the kinetic theory of gases in which particles diffuse into empty spaces. In the kinetic theory such diffusion arises from random walk

dynamics arising from collisions. In liquid fluidized beds collision dynamics do not dominate because there is a substance between the particles which keep them from touching. There is a dispersive action to hydrodynamic interaction of particles in Newtonian liquids which is obvious in experiments and direct simulation of particles large enough to see; but there does not seem to be a tendency for particles to diffuse into empty places, in fact they fall in clusters. Probably collisions do dominate in gas fluidized beds of heavy particles at high fluidization velocities; the border between collision dominated and hydrodynamic dominated particle-particle interactions has yet to be defined. Batchelor acknowledges that hydrodynamic interactions will keep the particles from actually colliding but believes that velocity fluctuations might arise from variations in the configuration of particles and the resulting hydrodynamic interactions or, in the case of high Reynolds number flow around a particle, from turbulence in the fluid. Whether or when the fluctuation level is large enough to produce diffusion of particles into empty spaces is an open question.

After all the approximations are made, Foscolo and Gibilaro 1984 and Batchelor 1988 derive an equation like (VI.69) with explicit but apparently different coefficients. However, the diffusion parameter in Batchelor's theory is unknown; Batchelor says it is known only up to an order of magnitude and this parameter enters directly into his criterion for instability so that Batchelor's theory can be compared with experiments only in a qualitative sense. The predictions of the Foscolo-Gibilaro theory are quite definite and are compatible with observations of bubbling but these observations do not define the onset of bubbling sharply.

Joseph 1990b noted that if Foscolo-Gibilaro 1984 particle-phase pressure (VI.64) is interpreted literally, then

$$\frac{\partial \pi_s}{\partial Z} = -\frac{2}{3} d \frac{\partial F}{\partial Z} = -\frac{2}{3} d \left[ \frac{\partial F}{\partial \varepsilon} \frac{\partial \varepsilon}{\partial Z} + \frac{\partial F}{\partial V_s} \frac{\partial V_s}{\partial Z} \right] \tag{VI.71}$$

leading to a term proportional $\partial V_s / \partial Z$ which was not considered in other theories. When this term is factored into a stability calculation, uniform fluidization is always unstable. In fact, for particles large enough to see in water, void fraction waves perpendicular to the flow rather than bubbles can be seen and explained ultimately by the stable orientation of long bodies across the stream. I would not say that such flows are uniformly fluidized.

The purpose of this rather long digression into modeling of fluidized beds is not to promote one or the other model, but to show the reader how the models rest on unproven assumptions which might be tested by direct numerical simulation.

REMOVE THIS PAGE (only used to generate table of contents)